Title page

Type: Original Article

Title: Improving the spatial alignment in PET/CT using amplitude-based respiratory-gated PET and patient-specific breathing-instructed CT

Abbreviated title: Patient-specific breath-hold CT in PET

Authors: Charlotte S. van der Vos[1,2], Antoi P.W. Meeuwis[1], Willem Grootjans[3], Lioe-Fee de Geus-Oei [2,3], Eric P. Visser[1]

[1]Department of Radiology and Nuclear Medicine, Radboud university medical center, Nijmegen, The Netherlands

[2]University of Twente, Enschede, The Netherlands

[3]Department of Radiology, Leiden University Medical Center, Leiden, The Netherlands

Institutions where the work was performed:

Department of Radiology and Nuclear Medicine, Radboud university medical center, Nijmegen, The Netherlands

Correspondence: Charlotte van der Vos, PhD.
Department of Radiology and Nuclear Medicine
Radboud university medical center
P.O. Box 9101, 6500 HB Nijmegen, The Netherlands
Phone: +31 06 11 76 34 05
E-mail: charlotte.vandervos@radboudumc.nl

Disclosure: Charlotte van der Vos received an educational grant during the writing of this manuscript from Siemens Healthcare, the Hague, The Netherlands.

Article statistics:

Abstract: 344

Article: 5087

References: 20

Figures: 4

Tables: 2

Abstract

Appropriate attenuation correction is important for accurate quantification of standardized uptake values (SUVs) in positron emission tomography (PET). Patient respiratory motion can introduce a spatial mismatch between respiratory-gated PET and computed tomography (CT), reducing quantitative accuracy. In this study, the effect of a patient-specific breathing-instructed CT protocol on the spatial alignment between CT and amplitude-based optimal respiratory-gated PET images was investigated.

Method: ^{18}F-fluorodeoxyglucose (FDG) PET/CT imaging was performed in 20 patients. In addition to the standard low-dose (LD) free-breathing CT, a breath-hold CT was acquired. The amplitude limits of the respiratory-gated PET were used to instruct patients to hold their breath during CT acquisition at a similar amplitude level. Spatial mismatch was quantified using the position differences between the lung-liver transition in PET and CT images, the distance between PET and CT lesions' centroids, and the amount of overlap as indicated by the Jaccard similarity coefficient (JSC). Furthermore, the effect on attenuation correction was quantified by measuring SUVs, metabolic tumor volume (MTVs) and total lesion glycolysis (TLGs) of lung lesions.

Results: All patients found the breathing instructions feasible, however 4 patients had trouble complying to the instructions. In total, 18 patients were included. The average distance between the lung-liver transition between PET and CT was significantly reduced for breath-hold CT (1.7±2.1 mm), compared to standard CT (5.6±7.3 mm) (P=0.049). Furthermore, the mean distance between the lesions'

centroids on PET and CT was significantly smaller when comparing breath-hold CT (3.6±2.0 mm) to standard CT (5.5±6.5 mm) (P=0.040). Quantification of lung lesion SUV was significantly affected, with a higher SUV_{mean} when breath-hold CT (6.3±3.9 g/cm^3) is used for image reconstruction, compared to standard CT (6.1±3.8 g/cm^3) (P=0.044). Though MTV was not significantly different, TLG reached statistical significance.

Conclusion: Optimal respiratory-gated PET in combination with patient-specific breathing-instructed CT results in an improved alignment between PET and CT images and shows an increased SUV_{mean} and TLG. Even though the effects are small, a more accurate SUV and TLG determination is of importance for a more stable PET quantification, which is relevant for radiotherapy planning and therapy response monitoring.

Keywords: amplitude-based optimal respiratory gating, lung tumors, image quantification in PET, spatial alignment, breath-hold CT

Introduction

Since the introduction of hybrid PET/CT imaging, there have been attempts to improve the alignment between PET and CT images (*1-4*). Appropriate spatial matching is of importance for accurate anatomical localization of radiotracer uptake, essential for adequate diagnosis and staging of a disease (*2,5*). Besides visual interpretation, CT scans are used for the attenuation correction of the PET data (*1,2,6,7*), where a mismatch can result in quantitative inaccuracies (*8*). This can be particularly problematic for lesions located near structures with large differences in density, for instance lung lesions. Accurate image quantification is the first step for using PET for personalizing medicine, providing the ability to more adequately plan therapy and monitor treatment response (*2,9-11*).

Particularly in thoracic and abdominal PET/CT imaging, issues regarding spatial overlap between the two image-sets arise due to respiratory motion. Respiratory motion in PET results in quantitative inaccuracies due to the blurred appearance of moving structures, which need to be corrected (*1,6,7,10,12*). A CT acquisition takes only several seconds and can therefore already be considered a respiratory motion-free image (*1,6,7*). However, combining the respiratory-gated PET and the CT images is not always easy. Respiratory gating protocols result in a PET image at a certain time point during the respiratory cycle, which does not necessarily correspond to the phase in which the CT image was captured. Therefore, respiratory gating could further reduce the spatial alignment between PET and CT images, resulting in an under- or overestimation of the SUVs (*3,6,7,10,13*).

Even though breathing instructed CT protocols are the most straightforward approaches to improve the spatial alignment between respiratory-gated PET and CT images, the use of simple instructions can be difficult to implement for operators and patients, and can have variable results. Some studies report a clear improvement when breathing instructions were used (*8,13*), while other studies did not show an improvement (or yielded even worse results) (*14*). In order to overcome these discrepancies between simple breathing instructions and to gain more control over the exact respiratory amplitude at which the CT is acquired, the use of a patient-specific breath-hold CT protocol is proposed in this study. In this protocol, the respiratory signal is used for both the reconstruction of the amplitude-based respiratory-gated PET as well as patient-specific breathing instructions during the acquisition of the CT.

Materials and methods

Testing of the protocol

Before the start of the study, five patients were asked to perform two types of breathing instructions in order to check the feasibility of the acquisition protocol. These five patients received a standard PET/CT scan. For the first type of breathing instructions, patients were asked to breathe normally until they were instructed to hold their breath for 10 s. For the second type of instructions, which were performed at least one min later, the patients were asked to take a couple of deep breaths, after which they were asked to hold their breath during the same expiratory

phase and for the same duration of 10 s. For both types of instructions the respiratory signal was measured and used to determine the specific moment of the breath-hold instructions given by the operator. All five patients could comply with both types of breathing instructions without any difficulty. The first instructions were chosen because it was easier for the operator to determine the exact moment of the respiratory signal reaching the correct amplitude level, and secondly because the breathing pattern of the patients was more comparable to the breathing pattern during the PET acquisition.

Patients

The local Institutional Review Board (IRB) approved the protocol, and informed consent was obtained for all patients (including the patients that tested the breathing instructions). Twenty patients with suspected lung cancer were prospectively included in this study and received an ^{18}F-FDG PET/CT scan with an additional low-dose breath-hold CT scan. Patient characteristics are summarized in table 1. The administration of ^{18}F-FDG was non-linearly dependent on patient weight (*15*). The administered activity is given by

$$A = 0.036 \times m^2,$$

where A is the activity [MBq] and m the body mass [kg]. The mean administered activity (and standard deviation) was 210±105 MBq with a mean incubation time (and standard deviation) of 63±6 min.

PET acquisition and respiratory gating

A Biograph 40 mCT PET/CT scanner with an extended field of view (TrueV) was used (Siemens Healthcare, Knoxville, Tennessee, USA). This scanner is accredited by the Research 4 Life (EARL) initiative for quantitative PET/CT imaging (*16*). The PET images were acquired using an optimized, amplitude-based respiratory gating algorithm (HD•Chest) that was integrated in the PET/CT software. Respiratory gating was performed on bed positions covering the thorax and upper abdomen. Gated and non-gated bed positions were acquiring during free breathing for 6 and 2 min, respectively. Respiratory gating was performed with a duty cycle of 35%, providing a good balance between image quality and motion rejection (*7*). The longer acquisition time for the gated bed positions (thorax and upper abdomen) as compared to the non-gated ones led to images with similar statistical quality after gating. The respiratory signal was acquired using a respiratory gating system with a pressure sensor integrated in an elastic belt placed around the patient's abdomen (AZ-733V electronics, Anzai, Medical Co, Ltd., Tokyo, Japan).

PET image reconstruction

The PET images were reconstructed using a 3D ordered subset expectation (3DOSEM) algorithm with a spatially varying point spread function (TrueX) incorporating time-of-flight information (UltraHD PET). Image reconstruction was performed with 3 iterations and 21 subsets. The slice thickness of the PET images was matched with the ones of the attenuation CT. Post reconstruction filtering was performed using a 3D Gaussian filter kernel with a full width at half maximum of 3.0 mm. A transaxial matrix size of 400 x 400 (with pixel size of 2 x 2 mm) was

used for the PET reconstructions. All PET images were reconstructed using the respiratory-gating algorithm.

Standard LD CT protocol

A standard LD spiral CT (standard CT) was acquired with a free breathing protocol. The X-ray tube voltage was chosen using CARE kV, with a reference tube voltage of 120 kV. The tube current was modulated using CARE Dose4D, with a reference tube current of 50 mAs. CT images were made with 0.5 s rotation time, a pitch of 1, and 16 x 1.2 mm collimation. A reconstruction with an increment of 3.0 mm and a reconstructed slice thickness of 5.0 mm was made for the attenuation correction. To quantify the lung-liver boundary and to delineate the lung lesions, the anatomical CT with reconstructed slice thickness of 3.0 mm, a sharper reconstruction kernel, and smaller field of view, was used.

Patient-specific breathing-instructed CT protocol

During the additional LD spiral CT acquisition, the respiratory signal of the patient was measured and the PET amplitude range was used to provide specific breathing instructions for each patient. Before the start of the PET/CT scan the breathing protocol was practiced to make sure that all patients understood the breathing instructions and they could all hold their breath for at least 10 s.

The tube voltage was chosen using CARE kV, with a reference tube voltage of 100 kV. The tube current was modulated using CARE Dose4D, with a reference tube current of 35 mAs. These values were lower than the standard LD CT to reduce the radiation dose for the patient. Other acquisition and reconstruction settings were

similar to the two reconstructions of the standard LD CT, except for the higher pitch (1.5 instead of 1) to reduce scan time for the breath-hold protocol.

Breathing instructions

To analyse the effect of breathing instructions on the alignment between respiratory-gated PET and CT, patients that did not perform the breathing instruction correctly were excluded from analysis. Correct execution of the breath-hold protocol by the patient was determined by measuring the average breathing amplitude before the start of the CT scan and during the CT acquisition. The ratio between the two amplitudes was calculated to determine if the patient managed to comply with the instructions, which means that with a lower ratio less respiratory motion is present in the breath-hold CT image (see Figure 1 for a visual explanation of the used amplitude ranges).

Image Analysis

Analysis of the PET and CT images was performed using the Siemens Inveon Research Workplace 4.1 Software (Preclinical solutions, Siemens Medical Solutions, Knoxville Tennessee, USA). Spatial alignment between anatomy on PET and CT was quantified using four methods. First, quantification of spatial mismatch was performed by measuring the position differences for the liver dome in the craniocaudal direction. The liver dome was determined visually on the PET and CT images in the transaxial plane (using the lung setting for CT, window centre: -450 HU; width: 1500 HU). To quantify the alignment of the lung lesions, the lesions were delineated in the PET and CT images. In the PET images, lesions

were delineated using a fixed threshold region growing segmentation algorithm. The segmentation threshold was set to 40% of the SUV_{max}, which is recognized as a suitable threshold level for delineation of lung lesions (*17,18*). The lesions in the CT images were manually delineated using the lung setting. The alignment of the lesions was determined by quantifying the distance between PET and CT lesions' centroids (the second method), and third, the spatial overlap between de lesions on PET and CT was determined using the Jaccard similarity coefficient, defined as

$$J(VOI_{CT}, VOI_{PET}) = \frac{VOI_{CT} \cap VOI_{PET}}{VOI_{CT} \cup VOI_{PET}}.$$

In this equation, VOI_{CT} and VOI_{PET} denote the volume of interest determined on CT and PET respectively. For the fourth method the SUV (both SUV_{max} and SUV_{mean}), MTV and TLG were compared for both PET reconstructions to analyze the effect of spatial matching on quantification of radiotracer uptake.

Statistical analysis

Since not all the paired groups were normally distributed, statistical analysis was performed using the Wilcoxon Signed Ranks test using SPSS Statistics 20 (IBM, Chicago Illinois, USA). Statistical significance was defined for $p<0.05$. Data are reported as mean ± standard deviation.

Results

The average duration of the breath-hold protocol was 12.1±0.91 s. The protocol started with an average of 4 s time interval between the breath-hold instructions

and the start of the CT acquisition. This four second interval was caused by the standard delay before the CT scan and the observation time that was required to inspect whether the patient was able to comply with the instructions. The CT acquisition itself had an average duration of 8.0±0.55 s, with a scan range of 41.4±3.2 cm.

After practicing the breathing instructions (before the start of the PET/CT scan), all patients indicated that the instructions were feasible. Nevertheless, when patients appeared not to be able to comply with the instructions during the CT acquisition they were excluded from analysis, following the method described in the 'Materials and Method' section. When a cut-off value of 0.4 was used for the ratio between the average breathing amplitude before the start of the CT scan and during the CT acquisition 4 out of the 20 patients were excluded. A cut-off value of 0.4 was chosen to indicate that on average, the patients could effectively reduce the breathing amplitude by more than half during the end-plateau phase of the respiratory cycle. The average ratio for the group of patients who did comply with the breathing instructions was 0.17 (standard deviation: 0.11, range: 0.04-0.39), while the average ratio for the other four patients was 0.95 (standard deviation: 0.56, range: 0.59-1.78). Nevertheless, for 2 out of these 4 patients, the respiratory signals during the CT scan indicated that they did manage to hold their breath long enough to scan both the lungs and lung-liver boundary. When the respiratory signal until the acquisition of the lung-liver boundary was considered, the ratio for these two patients was lower than the cut-off value. Although these two patients did not manage to hold their breath during the entire CT acquisition, the area of interest was covered during the breath-hold period and the data were eligible for analysis.

The data of the other two patients were not included in this study. In Figure 2 the amplitude ratios of the individual patients is shown. For the remaining 18 patients, 17 lung-liver boundaries were determined and 31 lesions were delineated. For one patient the lung-liver boundary could not be measured on CT due to the presence of pleural effusion.

The results of this study are shown in Table 2, and an example of a patient scan is shown in Figure 3. A significant improvement in the position difference on PET and CT is detected between the lung-liver boundary when using the breath-hold CT (1.7±2.1 mm), versus the standard CT (5.6±7.3 mm) (P=0.049). For 5 patients, the difference of the lung-liver boundary between PET and standard CT is more than 5 mm, with an average distance of 15.6±5.0 mm. For these five patients the PET in combination with the breath-hold CT shows improved matching in lung-liver boundary, with a mean distance of 1.8±1.6 mm.

The difference in spatial match of the lesions between gated PET and the standard and breath-hold CT images show mixed results, even though there is a statistically significant improvement for the distance between the centroids of the lesions between PET and the breath-hold CT (3.6±2.0 mm) and standard CT (5.5±6.5 mm) (P=0.040). There are 9 lesions in the standard CT group with a distance more than 5 mm. For 8 of these lesions the difference in centroids location improves when the breath-hold CT is used in combination with the respiratory gated PET, see Figure 4. However, the Jaccard similarity coefficient shows no significant improvement when breath-hold CT is compared to the standard CT group.

There is a statistically significant difference in radiotracer uptake when PET images are reconstructed using the standard compared to the breath-hold CT. The average SUV_{mean} increases from 6.1±3.8 mm for the standard CT images to 6.3±3.9 for the breath-hold CT images (P=0.044). SUV_{max} does not show a statistically significant difference between the two PET images (P=0.104), nor does the MTV (P=0.930). However, the TLG reached statistical significance, with a slight increment of 0.05±3.37 g for the PET scans reconstructed using the breath-hold compared to the standard CT, with a mean of 54.50±143.4 g and 54.55±143.4 g (P=0.018) for the standard and breath-hold reconstructed PET images respectively. Although the difference in SUV and TLG are minimal, the breath-hold CT group shows a consistently higher measurement compared to the standard CT group, resulting in the significant difference between the two groups.

The patients included in this study were all suspected for lung carcinoma, and eight of these patients also had diagnosed chronic obstructive pulmonary disease (COPD) (Gold I or II). Two out of 4 patients who could not comply with the breathing instructions had COPD. For this study the patients were instructed to hold their breath for an average of 12.1 s. For the 25 patients the success rate of the breath hold procedure was 92% (23 out of 25 patients), indicating that even for this patient cohort the breathing instructions of more than 10 seconds are feasible.

Discussion

This study shows that spatial alignment between PET and CT images is improved when patient-specific breathing instructions are provided during CT imaging. In this protocol, breathing instructions can be personalized to the individual patient while providing the operator the ability to objectively monitor the performance of the breath-hold manoeuvre. This study demonstrated improved control over the exact moment to perform the breath-hold manoeuvre compared to the commonly used end-expiratory breath-hold method. The technique is relatively easy to implement in clinical practice and results in minimal additional exposure of the patient to ionizing radiation.

However, not all patients could successfully comply with the current breathing protocol, which is an important aspect to consider in this patient population, given that a considerable amount of patients have respiratory disorders that can potentially limit the compliance with the breath-hold manoeuvres. To further improve the proposed method and increase the success rate of the patients holding their breath, the time required to perform the breath-hold manoeuvre should be shortened. Optimization of the CT acquisition protocol is a first important step. Scan parameters such as pitch, collimator settings, tube current and peak voltage, can be balanced to acquire CT images with sufficient image quality whilst reducing scan speed as much as possible. Furthermore, integration of the breathing protocol in the scanner hardware and software can assist in a more efficient initiation and execution of the protocol, preventing unnecessary delays when using external hardware and software, as utilized in the current protocol. Furthermore, in order to appropriately reconstruct the PET images, the CT scan range should match or extend the PET scan range. This can resulted in unnecessary long breath-hold CT

scans. This PET/CT scanner could only acquire PET images in step and shoot mode, where scanning of an additional bed position required extension of the CT scan rage. In a number of patients, the basal lung fields were positioned outside the second bed position and required the acquisition of an entire new third bed position. In these patients, the scan range of the breath-hold CT needed to be extended, resulting in longer acquisition times. However, several PET/CT scanners are on the market that are able to acquire data using continuous bed motion. When using PET/CT scanners with continuous bed motion, the range of the PET can be specifically adapted to the patient's anatomy, without recording an additional full bed position. This can significantly reduce the scan time for the breath-hold CT in these patients (*19*). Furthermore, in the current protocol, only the PET/CT operator receives feedback regarding the breath-hold manoeuvre. An interesting approach would be to provide the patient with either visual or auditory feedback, which can assist the patient in maintaining the required breath-hold amplitude. There are different systems available that can provide this feedback, most of which are already used for radiotherapy applications (*20*).

Over the years, several strategies have been proposed to reduce spatial mismatching between PET and CT images. Initially, breathing instructions were used during the PET acquisition to create a motion-free image that matched the CT acquisition (*2,13*). Although these methods have shown to be useful for reducing the spatial mismatch between PET and CT images, the focus our respiratory matching protocols have been directed towards modifying the CT acquisition, given that safeguarding statistical quality of the PET images is important. The advantage is that such approaches result in the best statistical quality of the PET

images and an optimal use of the PET data. Although breathing instructions are a relative easy way to improve the spatial match between PET and CT images, it is shown that breathing instruction typically have variable results (*8,13,14*). This study showed that monitoring the patient's respiration during the breath-hold manoeuvre reduced this variability and provided a more consistent result regarding the reduction of spatial mismatch between PET and CT.

Besides breathing instruction, several other methods have been proposed to improve the spatial alignment between CT and respiratory-gated PET. For instance different methods that influence the timing of the CT acquisition; respiratory-triggered CT (*12*), were the (sequential) CT is triggered to the respiration of the patient, or fully gated 4D CT protocols (*1,21*) in which an CT image is acquired during all phases of the respiration. However, the stability regarding respiratory tracking is still being investigated for the triggered CT approach, whilst full CT gating is not suitable for routine diagnostics given the high exposure of the patient to ionizing radiation. Other methods include the use of PET list-mode data to elastically transform the PET data to match the CT image (*22,23*). One of the advantages is that all the PET data can be used for the motion-free PET reconstructions, compared to only 35% of the PET data that was used for the reconstructions made in this study. The last method is increasingly being pursued, although still requires validation in larger clinical trials.

The clinical impact of the observed differences in image quantification between PET images would have been relatively modest, with limited effect on the SUV, MTV, and TLG values. Nevertheless, reducing the effect of spatial mismatch is an

important step towards more stable PET quantification. Improving quantitative accuracy is of great importance, since quantitative indices in PET are increasingly being used for therapy response monitoring and radiotherapy planning (*11*,*24*). Therefore, improving the reliability and reproducibility of PET image quantification is important. In this study, the maximum difference in SUV between matching and non-matching PET/CT is 36.5% and 31.5% for the SUV_{max} and SUV_{mean} respectively, which indicates that combining optimal respiratory-gated PET and breathing-instructed CT scan can considerably affect SUV quantification.

Conclusion

Optimal respiratory-gated PET in combination with patient-specific breathing-instructed CT results in an improved alignment between PET and CT images and shows an increased SUV_{mean} and TLG. Even though the effects are small, a more accurate SUV and TLG determination is of importance for a more stable PET quantification, which is relevant for radiotherapy planning and therapy response monitoring.

Financial disclosure

Charlotte van der Vos received a research grant from Siemens. The other authors declare that they have no competing interests.

References

1. Nehmeh SA, Erdi YE. Respiratory motion in positron emission tomography/computed tomography: a review. *Semin Nucl Med*. 2008;38:167-176.

2. Nehmeh SA, Erdi YE, Meirelles GS, et al. Deep-inspiration breath-hold PET/CT of the thorax. *J Nucl Med*. 2007;48:22-26.

3. Goerres GW, Kamel E, Seifert B, et al. Accuracy of image coregistration of pulmonary lesions in patients with non-small cell lung cancer using an integrated PET/CT system. *J Nucl Med*. 2002;43:1469-1475.

4. Goerres GW, Burger C, Kamel E, et al. Respiration-induced attenuation artifact at PET/CT: technical considerations. *Radiology*. 2003;226:906-910.

5. van der Gucht A, Serrano B, Hugonnet F, Paulmier B, Garnier N, Faraggi M. Impact of a new respiratory amplitude-based gating technique in evaluation of upper abdominal PET lesions. *Eur J Radiol*. 2014;83:509-515.

6. van der Vos CS, Grootjans W, Osborne DR, et al. Improving the spatial alignment in PET/CT using amplitude-based respiration-gated PET and respiration-triggered CT. *J Nucl Med*. 2015;56:1817-1822.

7. Grootjans W, de Geus-Oei LF, Meeuwis AP, et al. Amplitude-based optimal respiratory gating in positron emission tomography in patients with primary lung cancer. *Eur Radiol*. 2014;24:3242-3250.

8. Fin L, Daouk J, Morvan J, et al. Initial clinical results for breath-hold CT-based processing of respiratory-gated PET acquisitions. *Eur J Nucl Med Mol imaging*. 2008;35:1971-1980.

9. van Elmpt W, Hamill J, Jones J, De Ruysscher D, Lambin P, Ollers M. Optimal gating compared to 3D and 4D PET reconstruction for characterization of lung tumours. *Eur J Nucl Med Mol Imaging*. 2011;38:843-855.

10. Callahan J, Binns D, Dunn L, Kron T. Motion effects on SUV and lesion volume in 3D and 4D PET scanning. *Australas Phys Eng Sci Med*. 2011;34:489-495.

11. Boellaard R, Delgado-Bolton R, Oyen WJ, et al. FDG PET/CT: EANM procedure guidelines for tumour imaging: version 2.0. *Eur J Nucl Med Mol Imaging*. 2015;42:328-354.

12. Daouk J, Fin L, Bailly P, Meyer ME. Improved attenuation correction via appropriate selection of respiratory-correlated PET data. *Comput Methods Programs Biomed*. 2008;92:90-98.

13. Meirelles GS, Erdi YE, Nehmeh SA, et al. Deep-inspiration breath-hold PET/CT: clinical findings with a new technique for detection and characterization of thoracic lesions. *J Nucl Med*. 2007;48:712-719.

14. van der Vos CS, Grootjans W, Meeuwis AP, et al. Comparison of a free-breathing CT and an expiratory breath-hold CT with regard to spatial alignment of amplitude-based respiratory-gated PET and CT images. *J Nucl Med Technol*. 2014;42:269-273.

15. de Groot EH, Post N, Boellaard R, Wagenaar NR, Willemsen AT, van Dalen JA. Optimized dose regimen for whole-body FDG-PET imaging. *EJNMMI Res*. 2013;3:63.

16. FDG-PET/CT Accreditation. resEARch 4 Life: an EANM initiative. Available at: http://earl.eanm.org/cms/website.php?id=/en/projects/fdg_pet_ct_accreditation.htm. Accessed April 26, 2017.

17. Erdi YE, Mawlawi O, Larson SM, et al. Segmentation of lung lesion volume by adaptive positron emission tomography image thresholding. *Cancer*. 1997;80:2505-2509.

18. Grootjans W, Usmanij EA, Oyen WJG, et al. Performance of automatic image segmentation algorithms for calculating total lesion glycolysis for early response monitoring in non-small cell lung cancer patients during concomitant chemoradiotherapy. *Radiother Oncol*. 2016;119:473-479.

19. Acuff SN, Osborne D. Clinical Workflow Considerations for Implementation of Continuous-Bed-Motion PET/CT. *J Nucl Med Technol*. 2016;44:55-58.

20. Linthout N, Bral S, van de Vondel I, et al. Treatment delivery time optimization of respiratory gated radiation therapy by application of audio-visual feedback. *Radiother Oncol*. 2009;91:330-335.

21. Nehmeh SA, Erdi YE, Pan T, et al. Four-dimensional (4D) PET/CT imaging of the thorax. *Med Phys*. 2004;31:3179-3186.

22. Lamare F, Ledesma Carbayo MJ, Cresson T, et al. List-mode-based reconstruction for respiratory motion correction in PET using non-rigid body transformations. *Phys Med Biol*. 2007;52:5187-5204.

23. Sun T, Mok GS. Techniques for respiration-induced artifacts reductions in thoracic PET/CT. *Quant Imaging Med Surg*. 2012;2:46-52.

24. Grootjans W, de Geus-Oei LF, Troost EG, Visser EP, Oyen WJ, Bussink J. PET in the management of locally advanced and metastatic NSCLC. *Nat Rev Clin Oncol*. 2015;12:395-407.

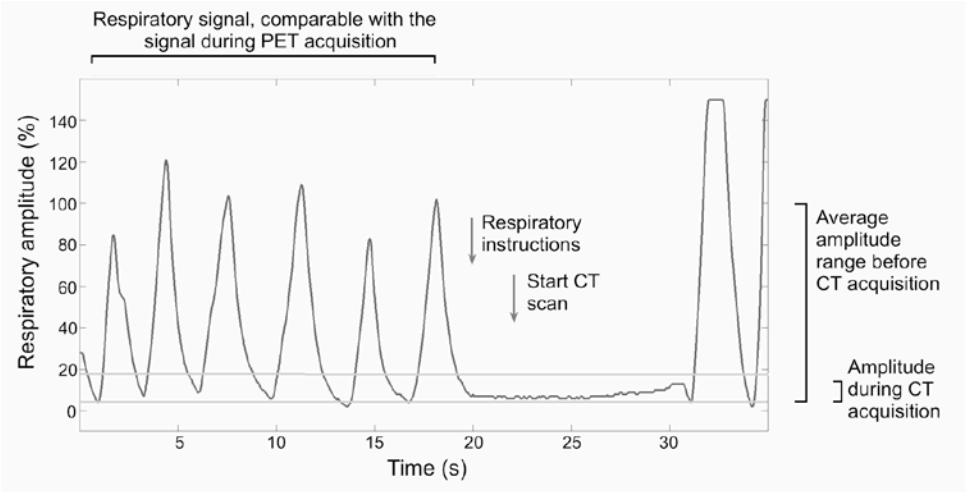

FIGURE. 1 Example of a respiratory signal before and during CT acquisition. Patients were instructed to hold their breath between the amplitude limits of the optimal PET gate (between the horizontal lines). To determine if the patient complied with the instructions, the amplitude range of the respiratory signal before the start of the CT scan (the mean amplitude range over several respiratory cycles), and during the breathing instructions were determined. The ratio between those two was used to determine whether the patients were able to hold their breath.

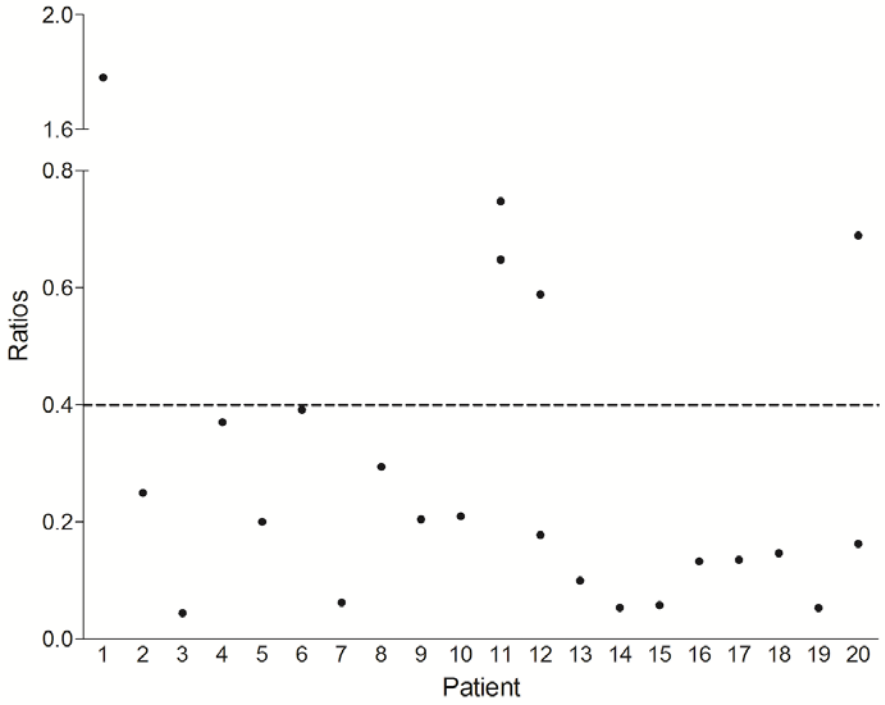

FIGURE. 2 The ratios between the average amplitude range of the respiratory signal during the breathing instructions and before the CT acquisition, for each patient. Patient 1, 11, 12 and 20 could not comply with the breathing instructions and show a higher ratio compared to the other patients. When only considering the amplitude during the CT acquisition of the lungs (and not including the upper abdomen region) the ratios of patient 12 and 20 improved, therefore they could be included in the data analysis. Patients 1 and 11 showed only a slight or no improvement, and were excluded from the data analysis.

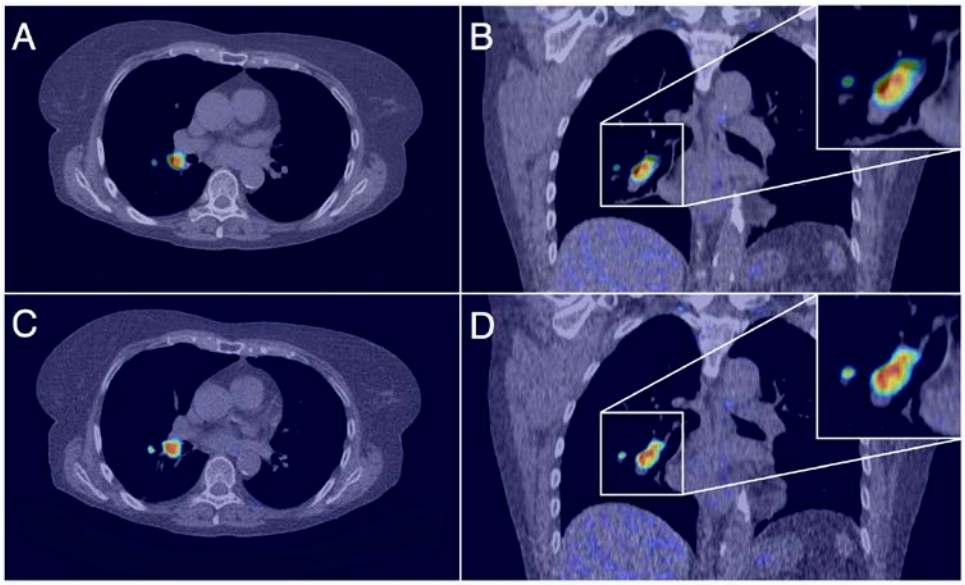

FIGURE. 3 Patient with small-cell lung cancer. The first row (A–B) depicts the transaxial (A) and coronal (B) plane of a standard CT fused with the respiratory-gated PET image. The second row (C–D) depicts the same transaxial (C) and coronal (D) place of the CT with breathing instructions and corresponding gated PET images. PET and breathing-instructed CT (C–D) show an improved match, whereas there is a mismatch for the PET and standard CT group (A–B).

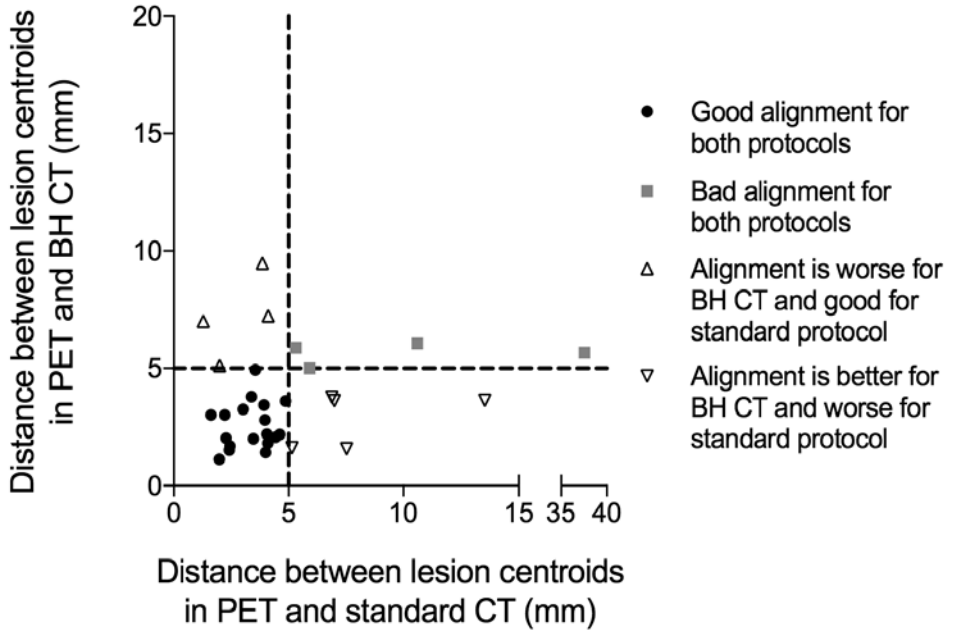

FIGURE. 4 Scatter plot showing results of the distance between centroids for lesions between PET and breath-hold CT, and PET and standard CT

TABLE 1. Summary of patient characteristics

	Value (SD)
Gender	
male	12
female	8
Mean age [years]	64.2 (9.2)
Mean weight [kg]	76.3 (18.1)
Mean administered activity [MBq]	210 (105)
Diagnosis	
Primary lung cancer	10
Metastasis	6
Other and unconfirmed	4
Location of lesion	
Upper lobes	16
Middle and lower lobes	9
Lung hilum	6

TABLE 2. Results (mean and standard deviations) of analyses of spatial alignment for both patient groups

	Standard CT and PET	Breath-hold CT and PET	P value
Mismatch of lung-liver boundary [mm]	5.6 ± 7.3	1.7 ± 2.1	0.049
Average distance between lesion centroids [mm]	5.5 ± 6.5	3.6 ± 2.0	0.040
Jaccard Similarity coefficient	0.32 ± 0.16	0.36 ± 0.16	0.176
SUV_{max} [g/cm^3]	10.3 ± 6.4	10.6 ± 6.6	0.104
SUV_{mean} [g/cm^3]	6.1 ± 3.8	6.3 ± 3.9	0.044
MTV	6.73 ± 15.6	6.69 ± 15.7	0.930
TLG	54.50 ± 143.4	54.55 ± 141.9	0.018